International Council for
the Exploration of the Sea

ICES C.M.1993/C:37
Hydrography Committee

Principles of inverse modeling of hydrographic data

by

J.C. de Munck

The Netherlands Institute for Sea Research,
Department of Physical Oceanography,
POBox 59,
1790 AB Den Burg,
The Netherlands

Abstract

An inverse modeling technique is applied upon a new hydrographic data set of the Iceland basin. The goal is to compute the barotropic component of the velocity field, without assuming a level of no motion. From a simulation study on the Levitus data set it is concluded that the estimation procedure can be stabilized significantly when a new way of sampling is used.

1 Introduction

In this paper the problem is addressed to estimate the geostrophic currents from hydrographic and tracer distribution measurements. The hydrographic data alone give a relationship between the vertical derivative of the horizontal velocity field and the density field. In the approach introduced by Wunsch (1978), the missing integration constants are found by an inverse model approach. Taking into account that some tracers are conservative, a set of mathematical equations can be obtained in which the integration constants act as the unknowns. A major difficulty is that the mathematical constraints resulting from the conservation assumptions are (almost) linearly dependent, yielding non-unique solutions. This non-uniqueness problem can be resolved by applying the Singular Value Decomposition (SVD) technique and filtering out the small scale variations.

In this paper a modified SVD-technique is (section 3) upon a new hydrographic data set of the Iceland basin. It was found (section 4) that the calculated transports are rather sensitive to variations of layer thickness, rounding off criterion and the number of 'boxes' used simultaneously in the inverse calculations. In section 5 a simulation study is performed on an alternative way of sampling which yields more stable equations.

2 Assumptions

The sampling scheme of hydrographic data intended for inverse modeling usually consists of a set of vertical sections which enclose one or more water volumes (boxes). At the vertical boundaries of these boxes the *in situ* density ρ and the geostrophic shear $\tilde{v}(s,p)$ are determined from temperature and salinity measurements as a function of pressure p. If s is the horizontal coordinate along a section, then the geostrophic flow perpendicular to the curve γ: $x=x(s)$, $y=y(s)$ is given by

$$v(s,p) = \frac{1}{f}\frac{\partial}{\partial s}\left\{ \int_{p_0}^{p} \frac{dp'}{\rho(s,p')} - g\,\zeta(s) \right\} \quad . \qquad (1)$$

Here $\zeta(s)$ is the unknown height of an arbitrary pressure level p_0. The positive flow direction of v with respect to the curve is to the right hand side for increasing s. The height of the sea level is obtained from a mathematical model describing the tracer concentrations. If it is assumed

that the tracer is stationary on time scales much larger than the flushing time and that the diffusivity is much smaller than the horizontal advection, the net amount of tracer material flowing into a box is zero:

$$\iint_{S^{(n)}} C\,\vec{v}\cdot d\vec{\sigma} = 0 \quad . \tag{2}$$

Here, $S^{(n)}$ is a part of the vertical box boundary on which the tracer varies from C_1 to C_2. The constants C_1 to C_2 should be chosen such that the enclosed layer is so thick that the vertical advection and diffusion are small compared to the horizontal advection. Equations in the form of Eq. (2) can only give restrictions in the barotropic component if there is a large bottom topography or an unstratified tracer, since otherwise Eq. (2) is automatically satisfied, due to the geostrophic degeneration.

3 The inverse model

Equation (2) is discretized by assuming that the barotropic part of the velocity field $\Diamond$ is constant between a station pair m. Its value is denoted by $\Diamond_m$ and the baroclinic part is denoted by $\tilde{v}_m(p)$. The following inverse equations for the barotropic flow can then be derived:

$$\sum_{m=1}^{M} a_{nm}\,\Diamond_m = b_n \quad , \tag{3}$$

with

$$a_{nm} = \iint_{S_m^{(n)}} d\sigma \qquad \text{and} \qquad b_n = -\sum_{m=1}^{M} \iint_{S_m^{(n)}} \tilde{v}\, d\sigma \quad , \tag{4}$$

where $S^{(n)}$ is partitioned into parts $S_m^{(n)}$, corresponding to the station pairs $m=1,\ldots,M$.

In a realistic measurement situation, it might happen that equations are contradicting each other, so that no solutions exist at all even if there are more unknowns than equations. This problem is solved by adding a noise term which accounts for the model mis-fit. In matrix form this can be expressed as follows:

$$A\Diamond = \mathbf{b} + \varepsilon \quad . \tag{5}$$

When $|\varepsilon|^2$ is minimized, at least one solution of the problem exists. But since many tracers may have a very similar distribution, the 'inverse equations' will be linearly dependent and the solution is non-unique. The complete class of solutions can be obtained from the SVD of the matrix A,

$$A = U \Lambda V^T \quad . \tag{6}$$

The matrix V is square and orthonormal: $V^T V = V V^T = I_M$ and Λ is a square diagonal matrix with non-negative numbers (the singular values) on the diagonal, ordered in decreasing order. Using the SVD, the general solution of the minimization problem is given by

$$\Diamond = V \Lambda^{-1} U^T \mathbf{b} + V_0 \mathbf{l} \quad . \tag{7}$$

Here the first term is a particular solution and the second term is the general solution of the homogeneous problem. Furthermore, Λ is obtained from Λ by replacing the zero's on the diagonal by infinite numbers, so that its inverses vanish. The matrix V_0 is that part of V corresponding to the vanishing singular values, so that $AV_0^T = 0$. By setting $\mathbf{l} = 0$ in (20) the minimum norm solution is found:

$$\Diamond_0 = V \Lambda^{-1} U^T \mathbf{b} \quad . \tag{8}$$

This solution is the one which minimizes the motion at the pressure level p_0. According to Wunsch (1978) this is the large scale solution, i.e. the solution which filters out the the small scale variations. However, a more direct way to remove the small scale variations, would be to minimize the differences in the geostrophic flows of subsequent station pairs:

$$H^2(\mathbf{v}) = \sum_j \frac{w_j}{P_j} \int_0^{P_j} dp \, [\, v_j^+(p) - v_j^-(p) \,]^2 \quad . \tag{9}$$

Here the summation is over all stations joining two station pairs. P_j is the maximum pressure of station j and w_j are arbitrary weighting constants. Furthermore, v_j^+ and v_j^- represent the total geostrophic velocities just before and just after station j.

When $\mathbf{v}$ is split into the baroclinic $\tilde{\mathbf{v}}$ and the barotropic flow $\hat{\mathbf{v}}$ one finds for $\hat{H}^2(\Diamond)$, the following expression in vector form,

$$\hat{H}^2(\Diamond) \equiv H^2(\tilde{\mathbf{v}} + \Diamond) = |D\Diamond + \mathbf{c}|^2 \quad , \tag{10}$$

with

$$D = \begin{bmatrix} w_1 & -w_1 & 0 & 0 & \\ & w_2 & -w_2 & & \\ & & \ddots & & \\ & & & w_J & -w_J \end{bmatrix} \tag{11}$$

and

$$c_j = \frac{w_j}{P_j} \int_0^{P_j} dp \, [\, \tilde{v}_j^{+}(p) - \tilde{v}_j^{-}(p) \,] \quad . \tag{12}$$

The problem of minimizing (10) under the condition that (3) is satisfied can be solved by using the general solution (7). After substituting (7) into (29), the value of **l** can be determined for which H is minimum. It is found that

$$\Diamond = \Diamond_0 - V_0 \, [V_0^T D^T D \, V_0 \,]^{-1} \, V_0^T D^T \, [D \, \Diamond_0 + \mathbf{c}] \quad . \tag{13}$$

In the derivation of (13) no use has been made of the specific form of D and **c** and the weights w_m. With these properties it can be shown that the total geostrophic flow, calculated with Eq. (13) is independent of the initial reference pressure p_0.

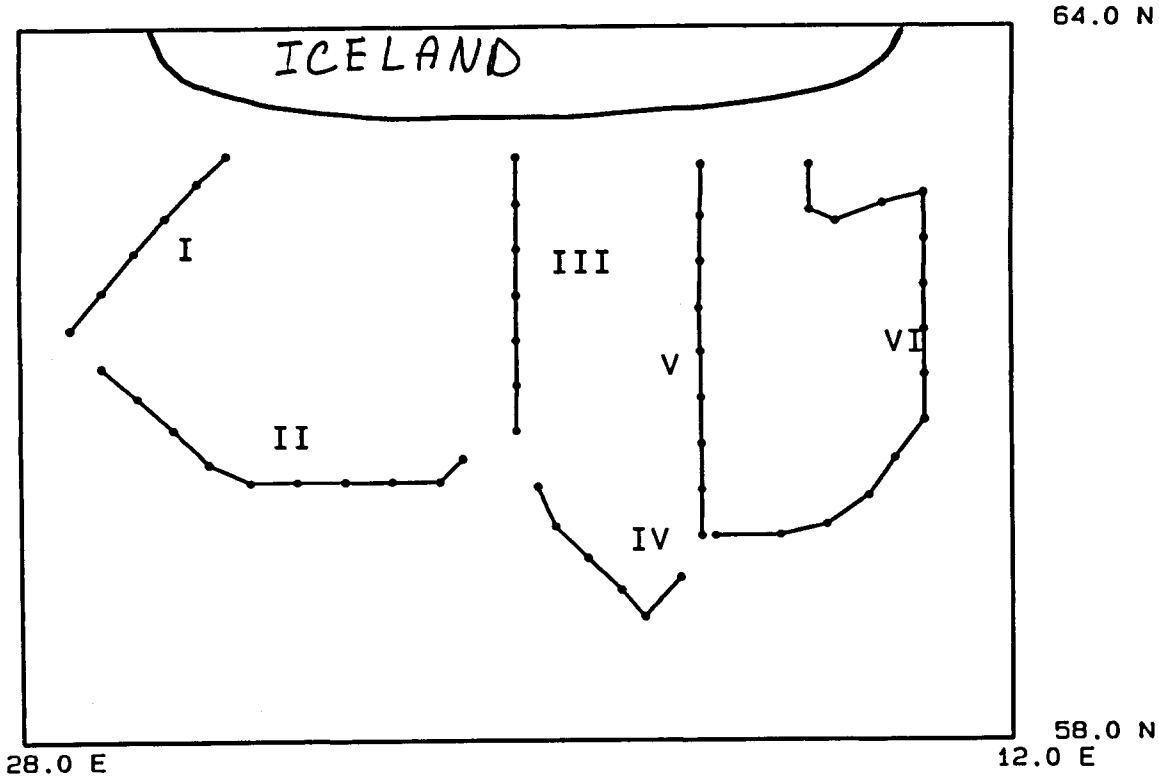

Figure 1. The area where the measurements were done. A dot represents a station, the connected dots represent the sections (numbered in Roman) through which the transports are calculated.

4 Results and Comparison

The data set used to demonstrate the methods derived in section 3 consists of CTD and tracer measurements performed in spring 1991, south of Iceland. In figure 1 the locations of the CTD-stations are indicated with dots. The line segments connecting the stations form three boxes on which the inverse model is applied. Figures 2 and 3 show the distribution of potential density, relative to the *0 dB* level. In figure 2 the isopycnals coincide with the separation of 'original water types'. In figure 3, on the other hand, the isopycnals are chosen such that the surfaces *S* are divided into parts of approximately equal width.

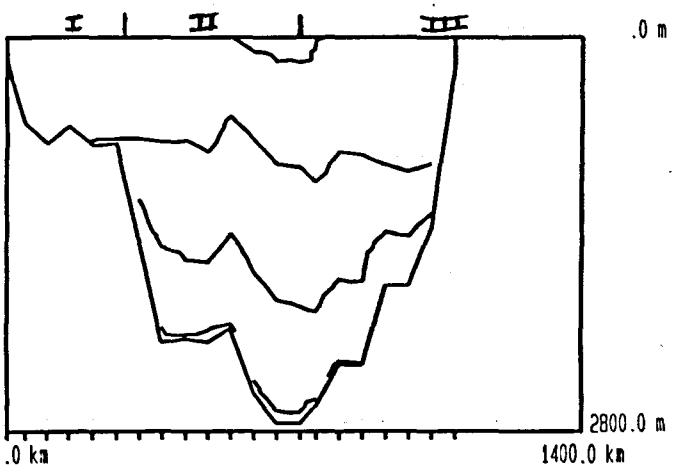

Figure 2. The isopycnals on the boundary of the left most box of fig. 1. The lines correspond to assumed original water types.

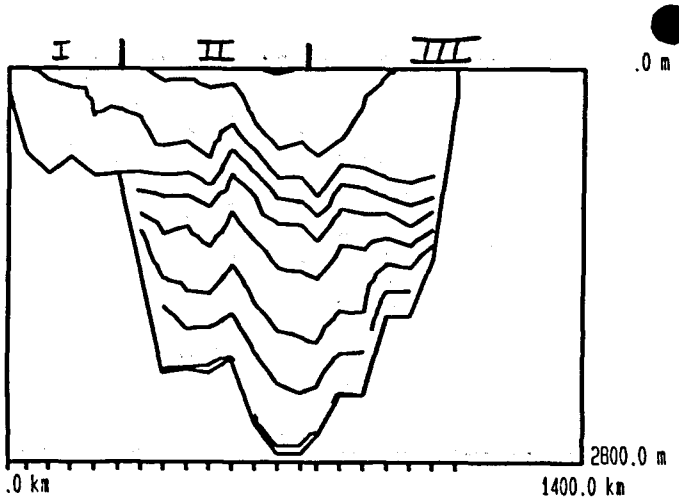

Figure 3. As fig. 2, but here it is attempted to create layers of equal thickness.

It is expected to find a northward current in the upper layer of the water column and a southward current at the bottom, carrying Overflow Water from the pole to lower latitudes. The size and the distribution of these currents is unknown. To answer these questions, the contours given in figure 1 are divided into *6* sections (numbered in Roman in figure 1) through which the transports are computed. The transports are computed for each of the water masses given in figure 2. To eliminate the effect of the Ekman layer, all water masses above *100 m* are disregarded.

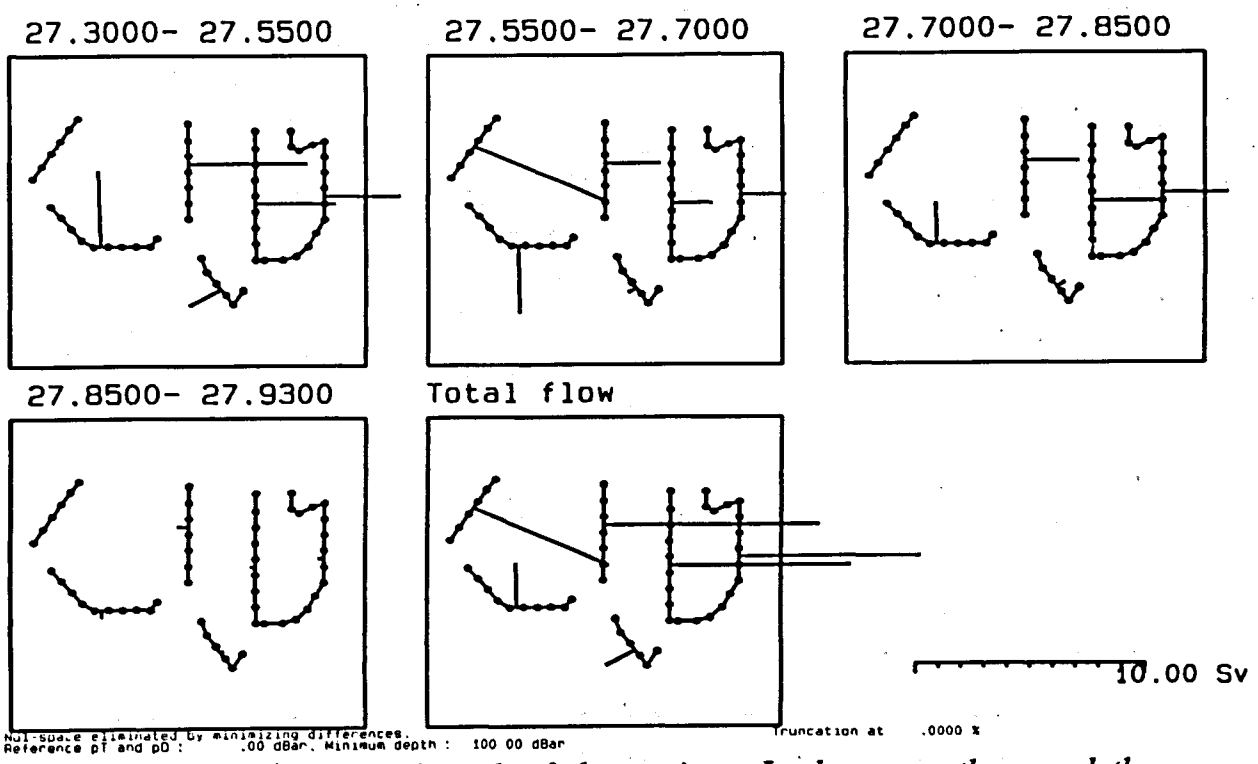

Figure 4. The flow through each of the sections. In the upper three and the lower left picture the transports are separated into the layers given by figure 2. In the lower middle picture the total transports through each of the sections is shown. In the lower right corner the scaling is shown.

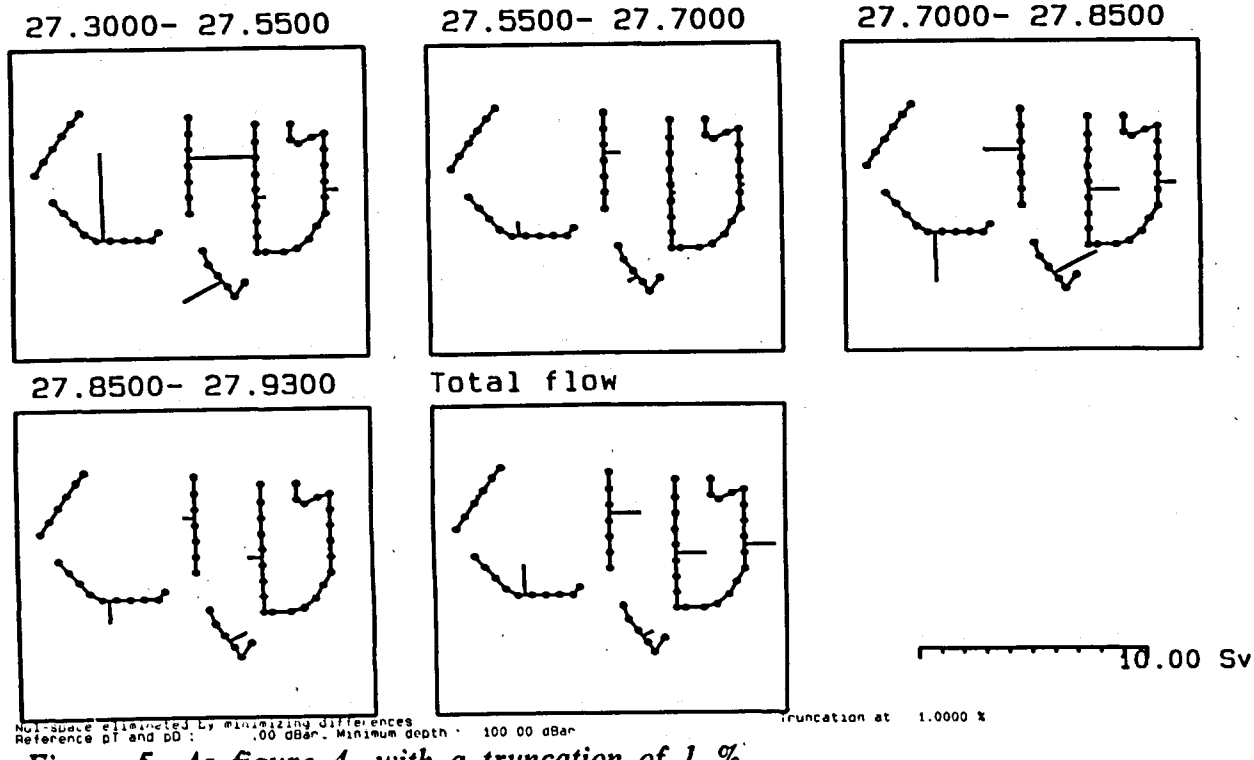

Figure 5. As figure 4, with a truncation of 1 %.

Figure 4 presents the first of our computations. The lower middle picture gives the total transports through each section. The inverse modeling equations are based upon the conservation of potential density and distribution of layers as given in figure 3. The ambiguity of the solution was removed by minimizing the vertically averaged differences in the velocities of subsequent station pairs, as described by Eq. (9). The absolute size of the flows quite large, e.g. the total eastward flow through section III equals *9.45 Sv*, according to our computations.

The cause of these large numbers is within Equation (7), as pointed out by Wunsch (1978), is that the small singular values blow up the solution. Since $\Sigma\ \lambda_k^2 = \mathrm{Tr}\{A^T A\}$, it is convenient to express the squares of the singular values as a percentage of the 'total power' of A, i.e., as a percentage of $\mathrm{Tr}\{A^T A\}$. To reduce the blow up effect the singular values smaller than the truncation level (usually *1%*) are set to zero. In this way the exact inverse equations are only approximately satisfied.

Figure 5 presents the transports computed similarly to those in figure 4, but with a truncation level of *1 %*. The total transport through section III is reduced to *1.38 Sv*. The effect of truncation can not simply be considered as a scaling of the transports. A comparison of figures 4 and 5 shows that the eastward transport through section I, present in figure 4 has disappeared in figure 5. With a truncation level of *.5 %* (not shown) , the transports were still quite large, but the distribution was rather different from figures 4 and 5.

A rather different picture (figure 6) is obtained when the distribution of the layers coincides with the assumed original water types, given in figure 2. Here the truncation level was taken at *1 %*. Compared to figure 5, the transport through section IV is enormously increased (up to *4.66 Sv*) whereas the total flow through section III is reversed in sign. The reference level of the potential density also has a significant effect on the resulting transports (not shown). When for instance the reference level is taken at *1000 dB*, the transport through section II is southward.

The direct SVD-technique yields sensitivities of the same order of magnitude as with the new approach presented here. But since the solutions obtained with SVD are dependent on an initial reference level, there is even one more parameter that may be varied. Using the interpretation of Veronis (1987), i.e. the level of no motion, it is natural to choose the reference level at ca. *1000 dB*. With $p_0 = 1000\ dB$ the agreement with figure 5 is rather good (not shown). Also the absolute values are in good agreement.

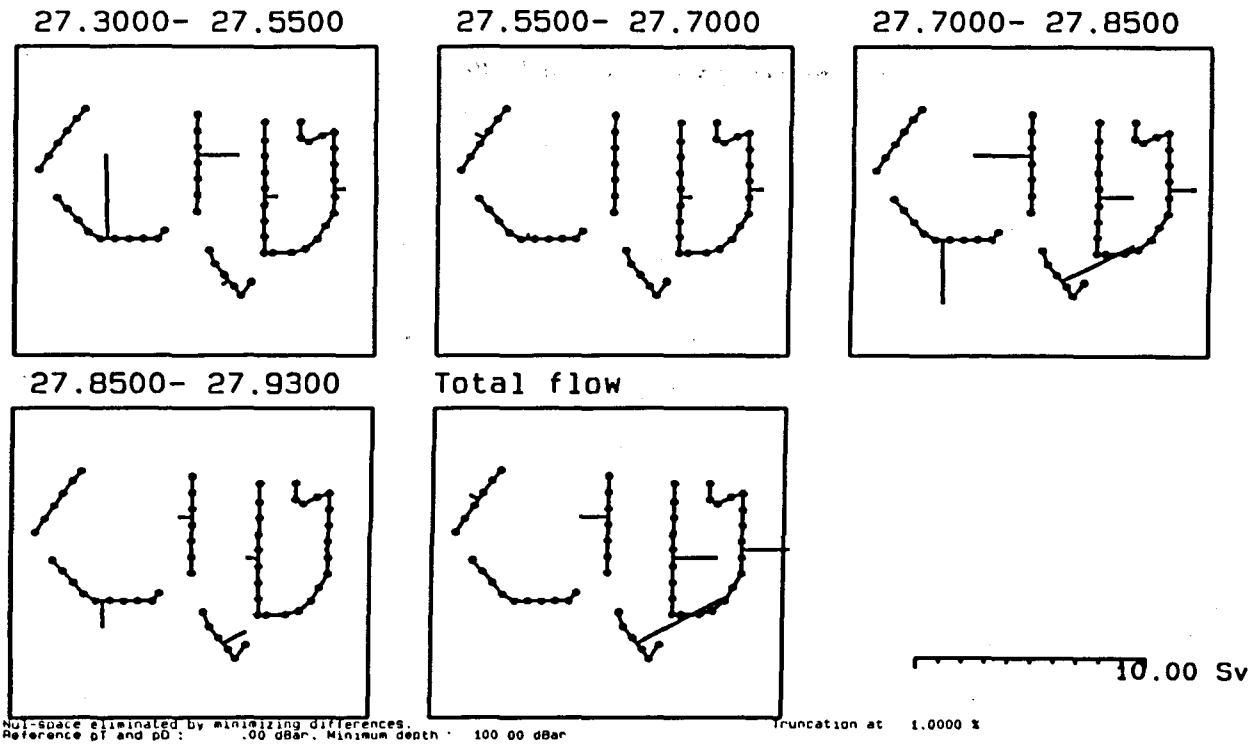

Figure 6. As figure 5, but here the layers were distributed according to the assumed original water types.

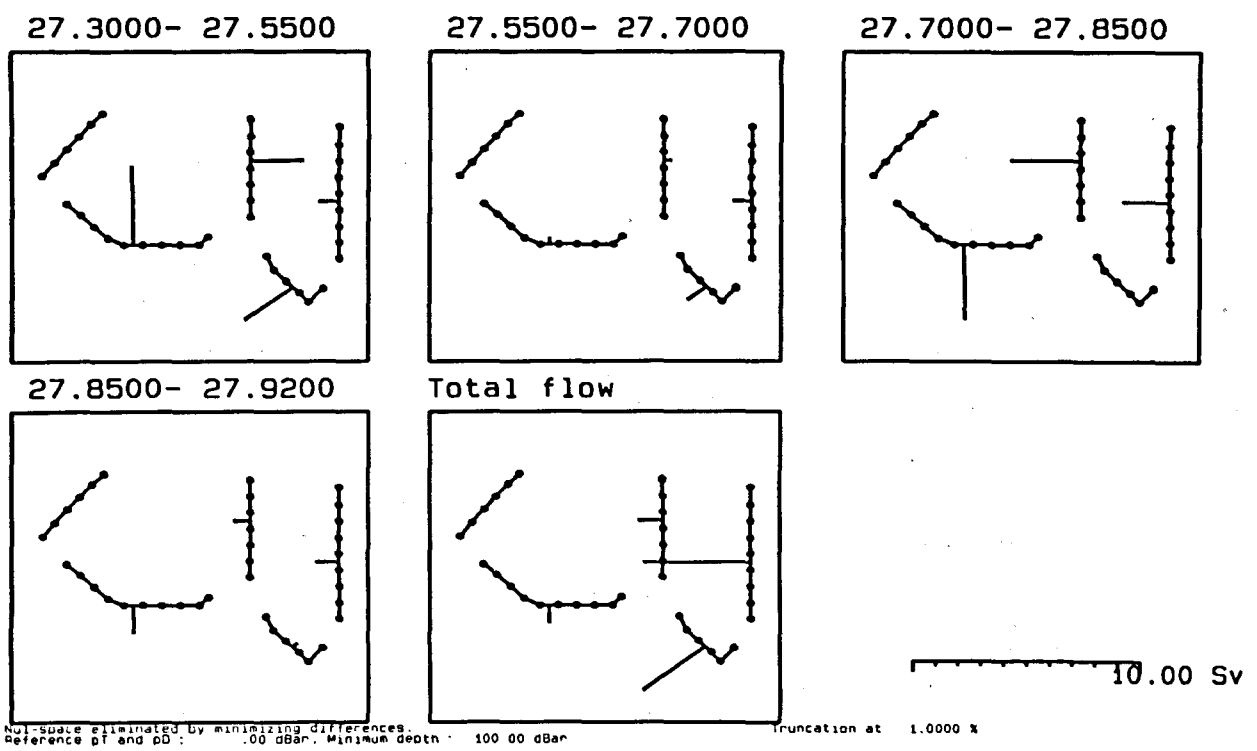

Figure 7. As figure 5, but here section VI was removed from the computations.

When section VI is left out of the computations, leaving two instead of three boxes, the eastward transport through sections III and IV disappears. Figure 7 shows the resulting transports for a truncation level of *1 %*. One may conclude from this result that the solution of the inverse modeling is not local: the solution at one place depends on the measurements at another place.

5 An alternative sampling strategy

From the above computations and comparisons it may be concluded that one can hardly extract quantitative information from the given data set on the basis of the geostrophic relations and the inverse modeling of conserved tracers. The central difficulty in the estimation procedure is that the inverse equations are too less restrictive to determine a unique solution. This becomes clear when the distribution of the singular values is considered. In all configurations considered (except figure 7) the distribution of the singular values is very similar to *47 %, 26 %, 11 %, 4 %, 3 %, 2%, ...* So there is only one independent equation per box at most and hence the distribution into layers does not yield additional independent information.

One might expect that a more favorable distribution of the data points is obtained when the number of boxes is large compared to the number of sections. Such sampling schemes are given in figure 8. The station positions coincide with the Levitus (1982) data set. For each triangular box only the total mass is assumed to be conserved and no division into layers is applied. In the case of figure 8A this gives *30* equations and *81* unknown flows. The distribution of the singular values of the matrix *A*, ordered from large to small is similar to: *7%, 7%, 6%, 6%, 5%, 5%, 4%, 4%, 4%, 4%, 4%,* etc. This shows that the inverse equations are much more independent than in the cases presented in section 4. Therefore, one may expect that if the transports through five surrounding sections are computed, the results will be more stable than in the conventional configuration.

Figure 9 shows the precise location of the sections and the corresponding transports, based on the minimization of flow differences. Although no truncation was applied, the maximum transport that occurred was only *2.2 Sv*, so that the 'blow up effect' present in the cases of the previous sections is diminished. Therefore, in this case there is no need to introduce a truncation parameter and study its effect. The results have a

clear interpretation: there is a superficial layer flowing to the north east and a return current at the bottom flowing in the opposite direction.

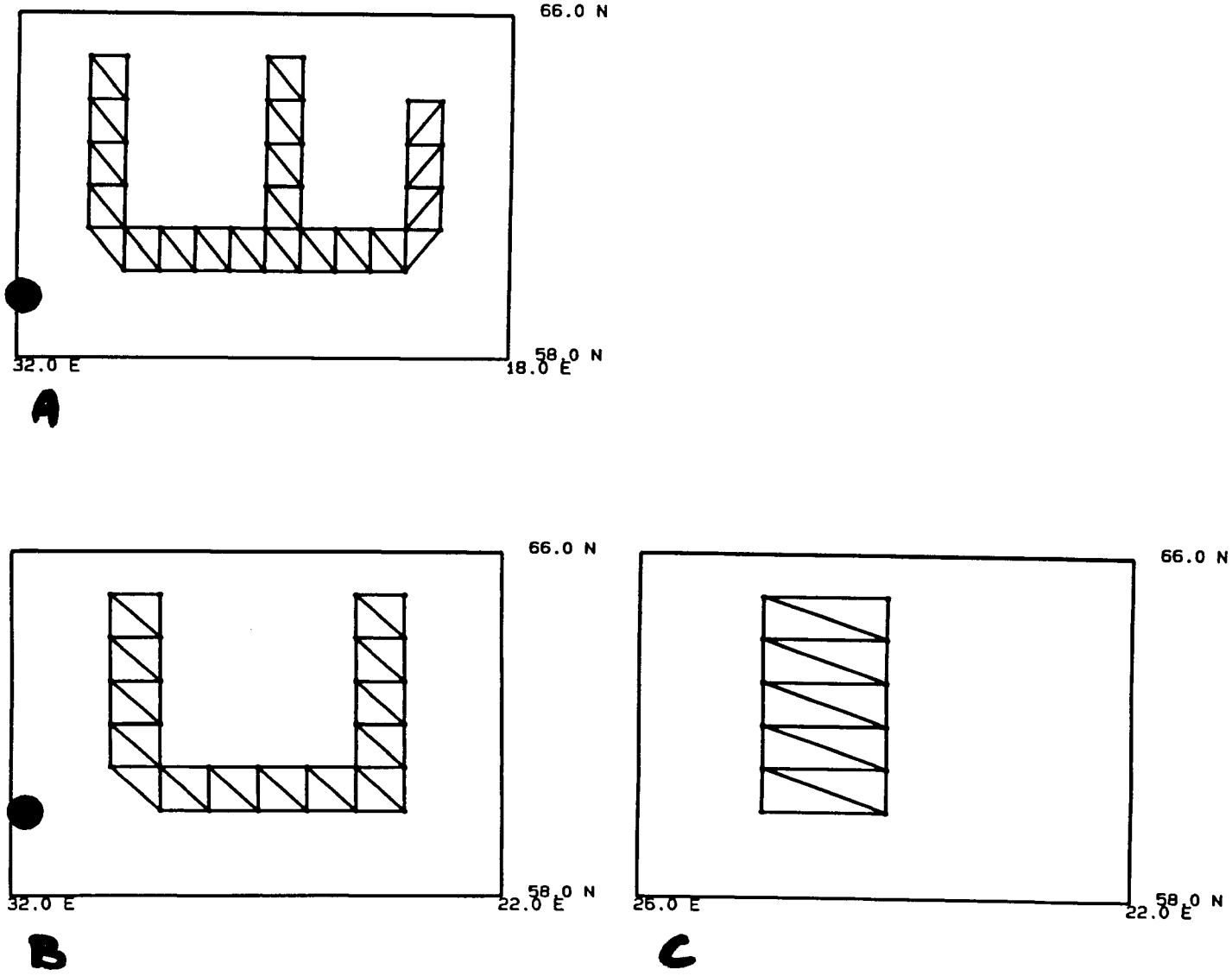

Figure 8. **A**: *An alternative way of sampling the same area as figure 2. By following a zigzag course, many more boxes can be created upon which the conservation principles can be applied. This results in many more independent equations.* **B**: *As* **A**, *but with leaving out the right branch.* **C**: *As* **A**, *but with leaving out the left and right hand side.*

In the conventional configuration, leaving out one box had a major effect on the solution. When in the alternative sampling scheme the right hand side was left out (figure 8B) or when both left and right hand side were left out (figure 8C), very similar qualitative and quantitative transports were obtained, see table 1.

layer	fig. 8A	fig. 8B	fig. 8C
1	*.60*	*.51*	*.62*
2	*-.11*	*-.13*	*-.13*
3	*-.40*	*-.49*	*-.43*
4	*-.48*	*-.62*	*-.49* *Sv*

Table 1. The effect of leaving out one or two branches of the sampling scheme, upon the distribution of transports through the middle section of figure 8. Transports are in Sv, positive flow is directed towards the east.

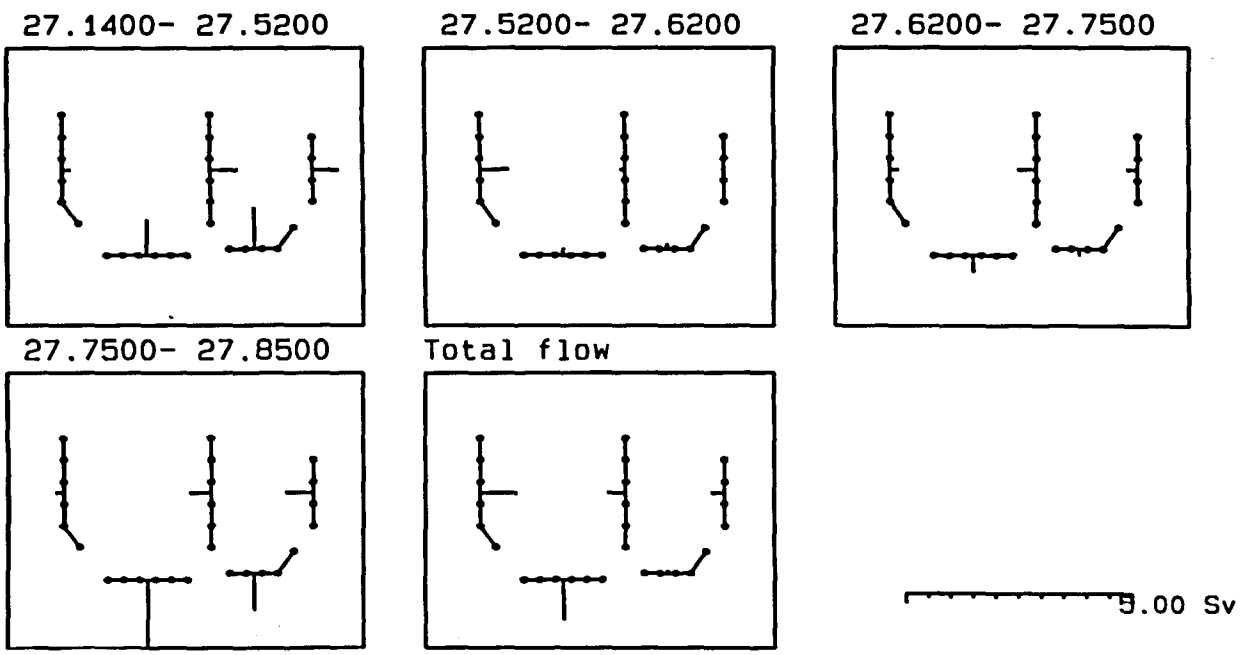

Figure 9. The resulting flows, when the alternative sampling scheme is used. The large scale solution was obtained by minimizing the differences in the flow field.

6 Discussion

The main issue raised in the present paper is the question whether it is possible to extract physically meaningful information from a linearly dependent set of inverse modeling equations. From the computations presented in this paper one may conclude that there are substantial limitations. On the other hand, the simulation studies with the alternative sampling scheme yielded physically relevant results, although the underlying system of equations is still formally underdetermined. The question is: how should one count the number of unknowns and the number of equations? If only the mass balance is taken into account for each box and if one assumes that the other equations are linearly dependent from it, then the number of equations equals the number of boxes. If for the number of unknowns one counts the number of station pairs, the mathematical system is underdetermined in either sampling scheme. But if, on the other hand the number of sections is counted one has an overdetermined system in the alternative sampling scheme and an underdetermined system in the conventional sampling scheme.

The alternative sampling scheme studied here has some similarity with the one used by Tziperman (1988). In that paper, a hydrographic data set consisting of a 2-D grid with half-degree spacing was used to study the oceanic circulation and mixing coefficients. This sampling scheme made it possible to include unknown mixing coefficients and to avoid a division of the water column into isolated layers in the inverse model. However, a full 2-D sampling scheme of the whole ocean is far beyond the practical possibilities. The sampling scheme studied in the present paper could be applied in practice by following a zigzag course and could therefore be realized more easily than a full 2-D sampling.

Compared to the 'ordinary' way of sampling, the alternative sampling scheme has the advantage that the data is more synoptic. It takes perhaps only half a day to perform three stations, the corners of the proposed boxes, and therefore it is much more likely that the data can be treated as synoptical than in the 'normal' case, where it may take more than a week to close a box. Other theoretical advantages are that 1.) the stability is obtained without assuming more than conservation of mass so that no division into layers is necessary and 2.) there is no need to truncate the SVD-solution which eliminates an important source of subjectivity. However, the author is well aware that the practical usefulness for real data, still has to be demonstrated.

7 Literature

Levitus S., 1982, *Climatological atlas of the world ocean*, NOAA Geophysical fluid dynamics laboratory professional paper No 13, Rockville, Maryland.

Tziperman E., 1988, *Calculating the time-mean oceanic circulation and mixing coefficients from hydrographic data*, J. Phys. Ocean., Vol. 18(3): 519-525.

Veronis G., 1987, *Inverse methods for ocean circulation*, in: *General Circulation of the Ocean*, H.D.I Abarbanel and W.R. Young (eds.), Springer, New York, pp. 102-133.

Wunsch C., 1978, *The North Atlantic general circulation West of* 50^0W *determined by an inverse method*, Rev. Geoph. Space Phys. 16(4):583-620.